3D-MICROPRINTED PDMS-BASED MICROFLUIDIC VESSELS FOR ORGAN-ON-A-CHIP APPLICATIONS

Xin Xu¹, Chen-Yu Chen², Ziteng Wen¹, Olivia M. Young¹, Bailey M. Felix², Bidhan C. Bandyopadhyay³, William E. Bentley², and Ryan D. Sochol^{1,2}

¹Department of Mechanical Engineering, University of Maryland, College Park, MD, USA

²Fischell Department of Bioengineering, University of Maryland, College Park, MD, USA

³Veterans Affairs Medical Center, Washington, D.C., USA

ABSTRACT

Microphysiological systems—also known as "organon-a-chip (OOC)" systems—hold considerable promise for applications including drug screening, disease modeling, and personalized medicine. A critical barrier to OOC efficacy, however, stems from manufacturing challenges that hinder the accurate recreation of 3D architectures and material properties of in vivo organ systems. To provide a new pathway to address these issues, here we leverage "Two-Photon Direct Laser Writing (DLW)" to 3D print physiologically relevant polydimethylsiloxane (PDMS) microvessels directly atop 3D microfluidic chipsfabricated via the "Vat Photopolymerization (VPP)" technique, "Liquid-Crystal Display (LCD)" 3D printing. Fabrication results revealed effective production of both interweaving and independent 3D microfluidic vessels with inner diameters (IDs) and wall thicknesses ranging from $80-100 \,\mu\text{m}$ and $5-10 \,\mu\text{m}$, respectively, as well as predesigned (i.e., as-printed) micropores with 5 µm diameters. Preliminary experimental results for MDA-MB-231 cells seeded within the porous microvessels revealed that the 3D PDMS system supported cell viability. In addition, pressure-vacuum experiments revealed that the permeation effects could be tuned to regulate the microenvironmental conditions internal and external to the porous microvessels. In combination, this work serves as a fundamental proof of principle for establishing entirely new classes of 3D microphysiological systems for diverse OOC applications.

KEYWORDS

Additive Manufacturing, 3D Printing, Direct Laser Writing, Two-Photon Polymerization, Organ-on-a-Chip

INTRODUCTION

Microphysiological or "OOC" systems—i.e., technologies that recapitulate in vivo tissue- and organ-level physiology in vitro—offer distinctive potential for a wide range of biomedical applications [1-3]. Initially, OOC systems were fabricated via conventional microfabrication protocols, such as multi-layer soft lithography [4-6]. Unfortunately, such microfabrication methods typically suffer from geometric restrictions that lead to relatively planar in vitro system architectures that bear little resemblance to their fully 3D in vivo counterparts [7-9]. Additive manufacturing (or "3D printing") approaches provide an alternative route to overcome these geometric limitations for OOC fabrication [10]. In particular, the Jennifer Lewis group has developed "material extrusion" approaches that involve "direct ink writing (DIW)" of sacrificial materials (e.g., pluronic) that can be cast and then evacuated, thereby leaving behind empty vessels encapsulated in extracellular matrix (ECM) [11-13]. Due to the reliance on nozzles for material deposition, however, such protocols are poorly suited for OOC applications that demand, for example, fully interweaving microvessels (like those of the kidney) or vessels with tightly controlled circular IDs (e.g., $\leq 100 \ \mu m$), thin walls/membranes (e.g., \leq 10 μ m), and/or custom micropores. To enable such capabilities for OOC systems, the additive micro/nanomanufacturing approach, DLW, is uniquely suited [14-16].

CONCEPT

Here we present a hybrid additive manufacturing strategy (**Fig. 1**) that leverages recent developments for "ex situ DLW (esDLW)" [17-19] as well as photopolymer-

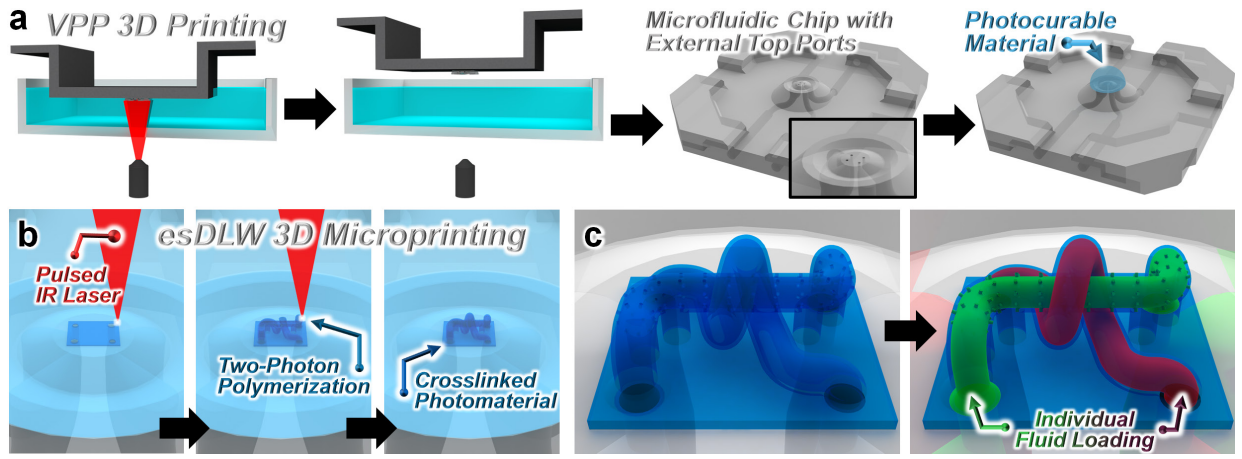


Figure 1. Conceptual illustrations of 3D interweaving microvessels fabricated via a hybrid micro-nanoprinting strategy. (a) "Vat Photopolymerization (VPP)" 3D printing of a microfluidic chip. (b) Point-by-point, layer-by-layer "ex situ Direct Laser Writing (esDLW)" 3D printing of interweaving microfluidic vessel structures using a PDMS-based photomaterial. (c) Example of selective microfluidic loading into the two independent microvessels.

izable PDMS [20] to achieve fully 3D microfluidic vessel structures of arbitrary design at biologically relevant length scales. First, the VPP approach, LCD 3D printing, is used to fabricate a bulk 3D microfluidic device with externally accessible outlet ports atop which PDMS-based photomaterial can be deposited (Fig. 1a). Second, esDLW is used to print 3D microfluidic vessel structures directly atop (and fluidically sealed to) the corresponding outlet ports of the DLP-printed microchip (Fig. 1b). Importantly, the designs of the 3D PDMS microvessels—e.g., IDs, wall thicknesses, circularity, tortuosity, and micropores—can be customized as desired. Lastly, following development and preparation for cell cultures, cell suspensions or other biological fluids can be loaded into (and retrieved from) the esDLW-printed microvessels via the input/output ports of the DLP-printed microchip for *in vitro* studies (Fig. 1c).

MATERIALS AND METHODS Microfluidic Chip Fabrication *via* "Vat Photopolymerization (VPP)"-Based 3D Printing

The bulk microfluidic chip was modeled using the computer-aided (CAD) software, SolidWorks (Dassault Systèmes, France). Each chip was designed with four ports at the sides that each connected to a corresponding top macro-to-micro interface port on the top of the chip (diameter = $100~\mu m$). Models were exported as STL files and imported into slicing software (CHITUBOX, China) for the ELEGOO Mars 3 3D printer (ELEGOO, China). The microfluidic chips were printed using Clear Microfluidic Resin v7.0a (CADworks, Canada). The prints were developed by rinsing with ethanol and drying with N₂ gas several times until fully cleared. Lastly, the prints were further cured under UV light for 30 s.

3D Microvessel Fabrication via "Ex Situ Direct Laser Writing (esDLW)"-Based 3D Printing

The various microfluidic vessel structures were modeled using SolidWorks (Dassault Systèmes). The interweaving vessels were designed with IDs of $80 \mu m$ and wall thicknesses of $10 \mu m$, while the independent microvessels were designed with IDs of $100 \mu m$ and wall thicknesses of $5 \mu m$; pre-designed micropores included diameters of $5 \mu m$. The models were exported as STL files and imported into the computer-aided manufacturing (CAM) software, DeScribe (Nanoscribe GmbH, Germany). The PDMS-based photoresist, IP-PDMS (Nanoscribe), was dispensed atop the top ports of the microfluidic chip (**Fig. 2a**), and the device was loaded into the Nanoscribe Photonic Profes-

sional GT2 3D printer with the $10\times$ objective lens and in the Dip-in Laser Lithography (DiLL) configuration. The esDLW process (hatching distance, layer height = 300 nm) was initiated with $15~\mu m$ of overlap with the top surface of the chip to enhance fluidic sealing. Following the esDLW process, the device assembly was developed by immersing it into 50 °C IPA for 30 min, fresh room temperature IPA for another 30 min, and then allowed to dry under ambient conditions. The device assembly was placed under UV light for 60 s to cure potential residual resin.

Optical Characterization

Micrographs captured during the *es*DLW printing process of the microvessels were carried out using the built-in Carl Zeiss Axio Observer inverted microscope (Zeiss, Germany) within the Nanoscribe Photonic Professional GT2 DLW 3D printer. Scanning electron microscopy (SEM) images were obtained using a TM4000 Tabletop SEM (Hitachi, Tokyo, Japan). Brightfield and fluorescence micrographs of experimental results were performed using a Macro Zoom Fluorescence Microscope System (MVX10, Olympus) coupled with X-Cite Illuminators for fluorescence illumination and a charge-coupled device (CCD) camera (DP74, Olympus) for recording.

Cell Experimentation

To prepare the device for cell testing, the device was immersed in ethanol and then DI water for 12 hrs each, followed by rinsing with fresh DI water for 1 min. The device exposed to oxygen plasma at 35 Watt for 60 s at a rate of 40 sccm using a Tergeo Plasma Cleaner (PIE Scientific, USA). Type I rat collagen coating solution (Sigma-Aldrich) was infused into the microvessels via the side ports of bulk microchip and incubated in a 37 °C CO₂ incubator for 1 hr. The system was then rinsed with both Phosphate Buffer Saline (PBS, Thermo Fisher Scientific) and Dulbecco's Modified Eagle's Medium (DMEM, Thermo Fisher Scientific). A suspension of MDA-MB-231 cells (1×10⁷ cells/mL) in culture medium (DMEM with 10% fetal bovine serum (FBS) and 1% penicillin/ streptomycin) was loaded into the vessel while 50 μ L of culture medium was dispensed on top of the microvessel (to prevent drying out during the incubation). The device was then placed in a covered petri dish and cultured in the 37 °C CO₂ incubator for 12 hrs. Cell viability was checked 2 days after cell seeding with InvitrogenTM LIVE/DEADTM Viability/Cytotoxicity kit (Thermo Fisher Scientific). The LIVE/DEAD staining solution (2 mM Calcein AM and

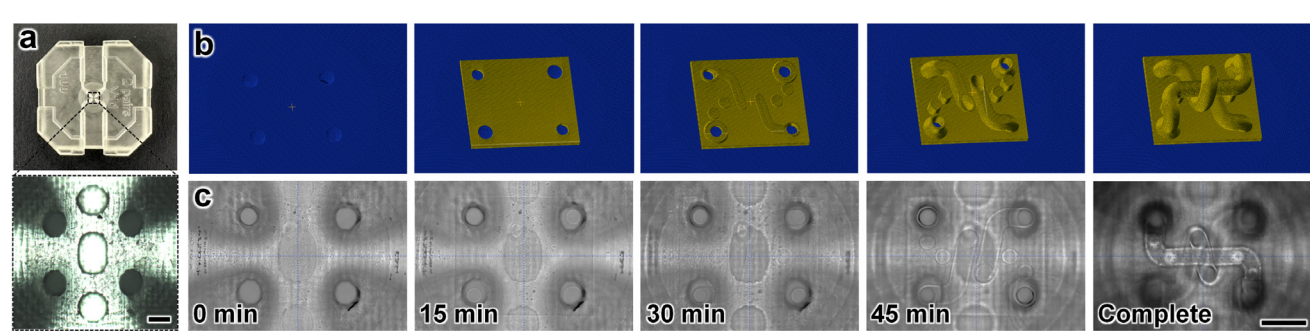


Figure 2. Fabrication results. (a) The LCD 3D-printed bulk microfluidic chip. Scale bar = $100 \mu m$. (b,c) The esDLW printing process for the interweaving PDMS microvessels. (b) Computer-aided manufacturing (CAM) simulations. (c) Corresponding esDLW 3D printing process. Total Print Time = 58 min; Scale bar = $250 \mu m$.

4 mM ethidium homodimer-1 (EthD-1) in PBS) was loaded into the microvessel and incubated for 30 min. The vessel structure was then cleaned with PBS before imaging.

Microfluidic Experimentation

Microenvironmental testing was performed using the Fluigent Microfluidic Control System (MFCS) and Flow Rate Platform and OxyGen software (Fluigent, France)—interfaced with the device ports *via* fluorinate ethylene propylene fluidic tubing (Cole-Parmer, Vernon Hills, IL) and stainless steel catheter couplers (Instech, Plymouth Meeting, PA). Positive input and output vacuum pressures for testing with 10% fluorescin-5-isothiocyanate (FITC) ranged from 0 to 20 kPa and 0 to 5 kPa, respectively.

RESULTS AND DISCUSSION Hybrid 3D Micro-Nanoprinting-Based Fabrication

The total LCD-based 3D printing process for the bulk microfluidic device was completed in under 30 min (**Fig. 2a**), with each batch print able to produce up to 12 chips simultaneously. CAM simulations and corresponding micrographs captured during the *es*DLW process for the interweaving microvessels are presented in **Figure 2b** and **2c**, respectively. The total *es*DLW printing process was completed in 58 and 38 min for the interweaving microvessels and the independent microvessel, respectively. SEM micrographs of representative fabrication results revealed effective production of the tortuous vessels as well as the pre-designed micropores (**Fig. 3**).

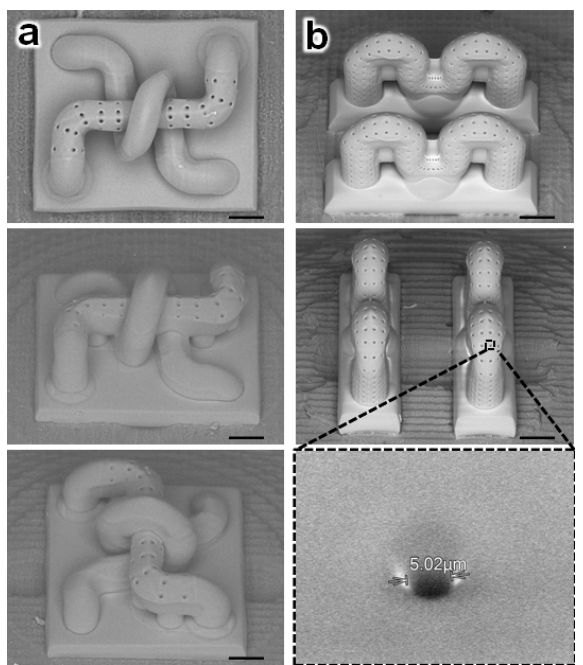


Figure 3. Fabrication results for microvessel structures. (a) Interweaving vessels. (b) Independent microvessel with expanded view of a micropore. Scale bars = $100 \mu m$.

Cell Loading and Viability

To evaluate the biocompatibility of the *es*DLW-printed PDMS-based microvessels (coated with type I collagen), we initially performed investigations of cellular adherence and cell viability using an epithelial cell line (MDA-MB-231, breast cancer cell line from adenocarcinoma). Experimental results for MDA-MB-231 cells

cultured on the inner lumen for 12 hrs revealed that the 3D PDMS microvessels were able to support cell adherence and viability (Fig. 4).



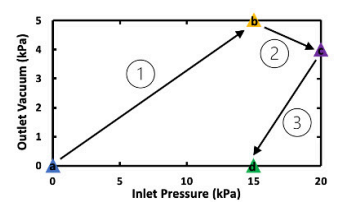
Figure 4. Results for cell experimentation. **(a,b)** Empty microvessel captured using **(a)** confocal brightfield, and **(b)** fluorescence microscopy. **(c)** Fluorescence micrograph of same vessel after culturing MDA-MB-231 cells on the inner lumen walls. Green = live cells. Scale bars = 100

Microfluidic Micropore-Mediated Permeation

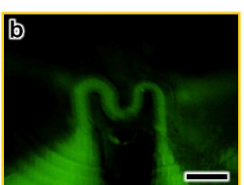
We also investigated the microenvironmental permeation dynamics of the microvessels facilitated by the predesigned micropores and tune via the pressures applied to the input and output. We immersed the system in DI water and then observed the infusion/permeation dynamics for 10% FITC while applying positive pressure at the inlet and negative pressure (vacuum) at the outlet. Initially, we did not observe any flow without applying pressure at either the inlet or outlet (Fig. 5a). We found that applying a positive pressure of 15 kPa at the inlet along with a vacuum pressure of 5 kPa at the outlet yielded mainstream flow that was retained within the microvessel (Fig. 5b). Vacuum application at the outlet was needed to prevent permeation through the arrayed micropores along the microvessel. For example, we observed that slightly larger pressure gradients between the inlet and the outlet, such as by applying a 20 kPa inlet pressure and a 4 kPa outlet vacuum pressure, resulted in partial external permeation near the portion of the microvessel closest to the inlet port (Fig. 5c). Furthermore, we found that in the absence of any vacuum pressure at the outlet, an outlet pressure of 15 kPa resulted in considerable external permeation of the FITC solution (Fig. 5d). These results suggest that both the input and output pressures can be regulated on-demand to tune the microenvironmental permeation dynamics to control internal-to-external chemical-molecular communications.

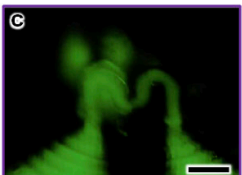
CONCLUSION

In this work, we introduced and demonstrated a novel hybrid strategy for additively manufacturing PDMS-based OOC systems with sophisticated 3D architectures at biologically relevant length scales. The presented OOC fabrication strategy—which combines VPP and esDLW 3D printing—offers unique means to circumvent the geometric restrictions of prior conventional soft lithography- and DIW-based approaches in recreating in vivo structures more accurately. Although LCD 3D printing was used in this work, alternative VPP (or potentially "material jetting" 3D printing approaches [21-23]) could be similarly employed for bulk microdevice production. The preliminary results suggest the PDMSbased microvessels can support cell/tissue culture and viability; however, future efforts are needed to continue evaluating such capabilities. Nonetheless, the presented results offer an important baseline for future works that extend the presented strategy to realize true-3D PDMSbased OOC systems with physiologically accurate









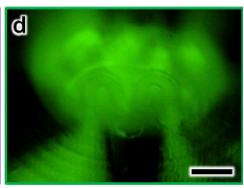


Figure 5. Experimental results for microenvironmental regulation. (a) No pressure/vacuum. (b) Retained mainstream flow. (c) Partial external permeation. (d) High external permeation. Scale bars = $250 \mu m$.

architectures that, ultimately, recapitulate *in vivo* tissueand organ-level physiology *in vitro*.

ACKNOWLEDGEMENTS

We greatly appreciate the contributions of members of the Bioinspired Advanced Manufacturing (BAM) Laboratory and the technical staff of Terrapin Works at the University of Maryland, College Park. This work was supported in part by U.S. National Science Foundation Award Number 1943356 and the National Science Foundation Graduate Research Fellowship Program under Grant No. DGE2236417. Any opinions, findings, and conclusions or recommendations expressed in this material are those of the authors and do not necessarily reflect the views of the National Science Foundation.

REFERENCES

- [1] D. J. Teixeira Carvalho, L. Moroni, and S. Giselbrecht, "Clamping strategies for organ-on-a-chip devices," *Nature Reviews Materials*, vol. 8, no. 3, pp. 147–164, 2023.
- [2] A. Bein *et al.*, "Nutritional deficiency in an intestine-on-a-chip recapitulates injury hallmarks associated with environmental enteric dysfunction," *Nature Biomedical Engineering*, vol. 6, no. 11, pp. 1236–1247, 2022.
- [3] C. M. Leung *et al.*, "A guide to the organ-on-a-chip," *Nature Reviews Methods Primers*, vol. 2, no. 1, 2022.
- [4] D. Huh *et al.*, "Acoustically detectable cellular-level lung injury induced by fluid mechanical stresses in microfluidic airway systems," Proceedings of the National Academy of Sciences, vol. 104, no. 48, pp. 18886–18891, 2007.
- [5] D. Huh *et al.*, "Reconstituting organ-level lung functions on a chip," Science, vol. 328, no. 5986, pp. 1662–1668, 2010.
- [6] S. N. Bhatia and D. E. Ingber, "Microfluidic organson-chips," Nature Biotechnology, vol. 32, no. 8, pp. 760–772, 2014.
- [7] H. J. Kim, D. Huh, G. Hamilton, and D. E. Ingber, "Human gut-on-a-chip inhabited by microbial flora that experiences intestinal peristalsis-like motions and flow," Lab on a Chip, vol. 12, no. 12, p. 2165, 2012.
- [8] K. J. Jang et al., "Human kidney proximal tubule-on-a-chip for Drug Transport and Nephrotoxicity Assessment," Integrative Biology, vol. 5, no. 9, pp. 1119–1129, 2013.
- [9] D. Huh et al., "Microfabrication of human organs-onchips," Nature Protocols, vol. 8, no. 11, pp. 2135– 2157, 2013.
- [10]B. Grigoryan et al., "Multivascular networks and functional intravascular topologies within

- Biocompatible Hydrogels," Science, vol. 364, no. 6439, pp. 458–464, 2019.
- [11] D. B. Kolesky *et al.*, "3D bioprinting of vascularized, heterogeneous cell-laden tissue constructs," Advanced Materials, vol. 26, no. 19, pp. 3124–3130, 2014.
- [12] K. A. Homan *et al.*, "Bioprinting of 3D convoluted renal proximal tubules on perfusable chips," Scientific Reports, vol. 6, no. 1, 2016.
- [13] N. Y. Lin *et al.*, "Renal reabsorption in 3D vascularized proximal tubule models," Proceedings of the National Academy of Sciences, vol. 116, no. 12, pp. 5399–5404, 2019.
- [14] A. Marino *et al.*, "A 3D real-scale, biomimetic, and biohybrid model of the blood-brain barrier fabricated through two-photon lithography (small 6/2018)," Small, vol. 14, no. 6, 2018.
- [15] A. T. Alsharhan, R. Acevedo, R. Warren, and R. D. Sochol, "3D microfluidics via cyclic olefin polymer-based in situ direct laser writing," Lab on a Chip, vol. 19, no. 17, pp. 2799–2810, 2019.
- [16] C. Michas *et al.*, "Engineering a living cardiac pump on a chip using high-precision fabrication," Science Advances, vol. 8, no. 16, 2022.
- [17] R. Acevedo *et al.*, "3D nanoprinted external microfluidic structures via ex situ direct laser writing," 2021 IEEE 34th International Conference on Micro Electro Mechanical Systems (MEMS), 2021.
- [18] O. M. Young *et al.*, "3D microprinting of multiactuator soft robots onto 3D-printed microfluidic devices via ex situ direct laser writing," 2022 Solid-State, Actuators, and Microsystems Workshop.
- [19] S. Sarker *et al.*, "3D-printed microinjection needle arrays via a hybrid dlp-direct laser writing strategy," Advanced Materials Technologies, vol. 8, no. 5, 2023.
- [20] N. Bhattacharjee, C. Parra-Cabrera, Y. T. Kim, A. P. Kuo, and A. Folch, "Desktop-stereolithography 3d-printing of a poly(dimethylsiloxane)-based material with Sylgard-184 properties," *Advanced Materials*, vol. 30, no. 22, 2018.
- [21] R. D. Sochol *et al.*, "3D printed microfluidic circuitry via Multijet-based additive manufacturing," Lab on a Chip, vol. 16, no. 4, pp. 668–678, 2016.
- [22] J. D. Hubbard *et al.*, "Fully 3D-printed soft robots with Integrated Fluidic Circuitry," Science Advances, vol. 7, no. 29, 2021.
- [23] B. Hayes, T. Hainsworth, and R. MacCurdy, "Liquid-solid co-printing of multi-material 3D fluidic devices via material jetting," Additive Manufacturing, vol. 55, p. 102785, 2022.

CONTACT

*X. Xu, tel: +1 (202)-957-2438; xuxin97@umd.edu